Supplemental Information: Machine Learned Synthesizability Predictions Aided by Density Functional Theory

Andrew Lee

February 15, 2022

Feature Name	Feature Importance
Stability	0.069
Formula minimum Covalent Radius	0.024
Formula maximum Mendeleev No.	0.021
Formula mode Covalent Radius	0.021
Tet/Oct E. Differences mode No. of p-valence e^-	0.009
Formula avg. dev. Covalent Radius	0.009
Formula mean No. of p-unfilled e^-	0.009
Tet/Oct E. Differences maximum No. of p-valence e^-	0.009
Tet/Oct E. Differences mean No. of p-valence e^-	0.009
Formula range Covalent Radius	0.008
Octahedral E. mode Electronegativity	0.008
Formula avg. dev. No. of p-valence e^-	0.008
Octahedral E. mode Column No.	0.008
Octahedral E. minimum Electronegativity	0.008
Formula mode Melting Temperature	0.008
Formula mean No. of p-valence e^-	0.008
Octahedral E. mean Electronegativity	0.008
Formula minimum Melting Temperature	0.007
Octahedral E. maximum Electronegativity	0.007
Tet/Oct E. Differences minimum No. of p-valence e^-	0.007
Formula mean Column No.	0.007
Formula maximum No. of p-valence e^-	0.007
Octahedral E. maximum No. of p-valence e^-	0.007
Formula mean groundstate band gap	0.007
Formula maximum Column No.	0.007
Formula range groundstate volume per atom	0.007
Octahedral E. mean No. of p-valence e^-	0.007
Formula avg. dev. groundstate band gap	0.006
Octahedral E. minimum Column No.	0.006
Formula range groundstate band gap	0.006
Octahedral E. minimum No. of p-valence e^-	0.006
Formula avg. dev. groundstate volume per atom	0.006
Formula maximum groundstate volume per atom	0.006
Octahedral E. mode No. of p-valence e^-	0.006
Formula avg. dev. Electronegativity	0.006
Formula mean Atomic Weight	0.006
Formula maximum No. of Valence e^-	0.006
Formula range No. of p-valence e^-	0.006
Octahedral E. mean Mendeleev No.	0.006
Octahedral E. mean Column No.	0.006
Formula mean No. of d-valence e^-	0.005
Octahedral E. maximum Mendeleev No.	0.005
Formula maximum groundstate band gap	0.005
Octahedral E. maximum Atomic Weight	0.005
Octahedral E. minimum No. of p-unfilled e^-	0.005
Octahedral E. mode Mendeleev No.	0.005
Octahedral E. minimum Mendeleev No.	0.005
Octahedral E. mode Atomic Weight	0.005
Octahedral E. mean Atomic Weight	0.005
Formula mean groundstate volume per atom	0.005
Formula mean Electronegativity	0.005
Octahedral E. maximum Melting Temperature	0.005
Tet/Oct E. Differences mean Melting Temperature	0.005

Tet/Oct E. Differences mean Mendeleev No.	0.005
Tet/Oct E. Differences maximum Mendeleev No.	0.004
Octahedral E. mean Number	0.004
Tet/Oct E. Differences mode Column No.	0.004
Tet/Oct E. Differences mean Electronegativity	0.004
Octahedral E. mode Number	0.004
Octahedral E. mean Covalent Radius	0.004
Tet/Oct E. Differences maximum Electronegativity	0.004
Formula mean Mendeleev No.	0.004
Octahedral E. minimum Number	0.004
Formula minimum Atomic Weight	0.004
Octahedral E. mean groundstate band gap	0.004
Tet/Oct E. Differences mean groundstate volume per atom	0.004
Formula minimum Number	0.004
Tet/Oct E. Differences maximum Melting Temperature	0.004
Tet/Oct E. Differences mode Mendeleev No.	0.004
Octahedral E. maximum Column No.	0.004
Formula range Melting Temperature	0.004
Formula minimum Electronegativity	0.004
Tet/Oct E. Differences mode Melting Temperature	0.004
Formula mode Number	0.004
Formula avg. dev. Melting Temperature	0.004
Tet/Oct E. Differences minimum Melting Temperature	0.004
Octahedral E. mean Melting Temperature	0.004
Formula mode Atomic Weight	0.004
Octahedral E. mode groundstate volume per atom	0.004
Octahedral E. maximum Space Group No.	0.004
Octahedral E. mode Melting Temperature	0.004
Octahedral E. maximum Number	0.004
Tet/Oct E. Differences minimum groundstate volume per atom	0.004
Formula mean Number	0.004
Tet/Oct E. Differences minimum Mendeleev No.	0.004
Tet/Oct E. Differences minimum Electronegativity	0.004
Formula mode Electronegativity	0.004
Octahedral E. minimum Melting Temperature	0.004
Octahedral E. maximum groundstate volume per atom	0.004
Octahedral E. minimum Space Group No.	0.004
Octahedral E. minimum Atomic Weight	0.004
Formula mean Space Group No.	0.004
Octahedral E. mode Space Group No.	0.004
Formula avg. dev. Mendeleev No.	0.004
Octahedral E. mean No. of p-unfilled e^-	0.004
Octahedral E. mode No. of p-unfilled e^-	0.004
Octahedral E. minimum groundstate volume per atom	0.004
Tet/Oct E. Differences mode groundstate volume per atom	0.004
Tet/Oct E. Differences mean Column No.	0.004
Tet/Oct E. Differences maximum groundstate volume per atom	0.004
Octahedral E. mode Covalent Radius	0.004
Octahedral E. mean groundstate volume per atom	0.003
Formula mean Melting Temperature	0.003
Octahedral E. minimum Covalent Radius	0.003
Octahedral E. maximum No. of p-unfilled e^-	0.003
Tet/Oct E. Differences mode Electronegativity	0.003
Formula avg. dev. Column No.	0.003

Octahedral E. minimum groundstate band gap	0.003
Tet/Oct E. Differences mode Space Group No.	0.003
Tet/Oct E. Differences maximum No. of p-unfilled e^-	0.003
Formula maximum Covalent Radius	0.003
Tet/Oct E. Differences mean Space Group No.	0.003
Formula range Electronegativity	0.003
Tet/Oct E. Differences mean No. of p-unfilled e^-	0.003
Tet/Oct E. Differences minimum Covalent Radius	0.003
Formula avg. dev. Space Group No.	0.003
Tet/Oct E. Differences minimum No. of p-unfilled e^-	0.003
Octahedral E. mode groundstate band gap	0.003
Tet/Oct E. Differences minimum Column No.	0.003
Formula mean Covalent Radius	0.003
Formula range Column No.	0.003
Octahedral E. maximum Covalent Radius	0.003
Tet/Oct E. Differences maximum Covalent Radius	0.003
Formula maximum No. of p-unfilled e^-	0.003
Tet/Oct E. Differences mean Covalent Radius	0.003
Tet/Oct E. Differences maximum Space Group No.	0.003
Tet/Oct E. Differences mode Covalent Radius	0.003
Tetrahedral E. mode Melting Temperature	0.003
Tet/Oct E. Differences maximum Column No.	0.003
Tet/Oct E. Differences minimum Space Group No.	0.003
Tetrahedral E. minimum Melting Temperature	0.003
Formula mode Mendeleev No.	0.003
Formula mean No. of Valence e^-	0.003
Formula mode Space Group No.	0.003
Formula maximum Number	0.003
Formula maximum Melting Temperature	0.003
Tetrahedral E. maximum Melting Temperature	0.003
Octahedral E. maximum groundstate band gap	0.003
Formula range Mendeleev No.	0.003
Octahedral E. mean Space Group No.	0.003
Tet/Oct E. Differences mode No. of p-unfilled e^-	0.003
Tet/Oct E. Differences minimum groundstate band gap	0.003
Formula range Space Group No.	0.003
Tet/Oct E. Differences mode groundstate band gap	0.003
Tet/Oct E. Differences maximum Atomic Weight	0.003
Tet/Oct E. Differences mean groundstate band gap	0.003
Formula maximum Atomic Weight	0.002
Octahedral E. maximum No. of Valence e^-	0.002
Formula range No. of p-unfilled e^-	0.002
Octahedral E. mode No. of Valence e^-	0.002
Formula minimum Mendeleev No.	0.002
Octahedral E. mean No. of Valence e^-	0.002
Formula minimum Space Group No.	0.002
Tetrahedral E. mean Mendeleev No.	0.002
Tetrahedral E. mode Mendeleev No.	0.002
Tetrahedral E. minimum Mendeleev No.	0.002
Tet/Oct E. Differences minimum Atomic Weight	0.002
Tet/Oct E. Differences maximum groundstate band gap	0.002
Formula avg. dev. No. of p-unfilled e^-	0.002
Tetrahedral E. mean Melting Temperature	0.002
Tet/Oct E. Differences mode Number	0.002

Tetrahedral E. maximum Electronegativity	0.002
Tet/Oct E. Differences mean Atomic Weight	0.002
Tet/Oct E. Differences mode Atomic Weight	0.002
Tetrahedral E. maximum Mendeleev No.	0.002
Octahedral E. mode No. of d-valence e^-	0.002
Tet/Oct E. Differences mean Number	0.002
Octahedral E. minimum No. of Valence e^-	0.002
Tetrahedral E. mode Electronegativity	0.002
Formula avg. dev. No. of Valence e^-	0.002
Tetrahedral E. minimum Electronegativity	0.002
Tet/Oct E. Differences maximum Number	0.002
Tetrahedral E. mode Column No.	0.002
Octahedral E. mean No. of d-valence e^-	0.002
Formula avg. dev. Atomic Weight	0.002
Tetrahedral E. mean Column No.	0.002
Tetrahedral E. minimum Column No.	0.002
Formula minimum groundstate volume per atom	0.002
Tetrahedral E. mean Electronegativity	0.002
Tetrahedral E. minimum Covalent Radius	0.002
Tetrahedral E. minimum groundstate volume per atom	0.002
Formula mean Row No.	0.002
Tet/Oct E. Differences minimum No. of Valence e^-	0.002
Tet/Oct E. Differences minimum Number	0.002
Tet/Oct E. Differences mode No. of Valence e^-	0.002
Formula range Number	0.002
Tet/Oct E. Differences mode No. of d-valence e^-	0.002
Tetrahedral E. minimum No. of Valence e^-	0.002
Octahedral E. minimum No. of d-valence e^-	0.002
Tetrahedral E. maximum Column No.	0.002
Formula range No. of Valence e^-	0.002
Tetrahedral E. maximum No. of Valence e^-	0.002
Tet/Oct E. Differences mode No. of Unfilled states	0.002
Octahedral E. maximum No. of d-valence e^-	0.002
Formula avg. dev. Number	0.002
Formula mode No. of Valence e^-	0.002
Octahedral E. mean No. of Unfilled states	0.002
Octahedral E. minimum Row No.	0.002
Tet/Oct E. Differences mean No. of d-valence e^-	0.002
Formula range Atomic Weight	0.001
Tetrahedral E. mean No. of Valence e^-	0.001
Tetrahedral E. mode groundstate volume per atom	0.001
Octahedral E. mean Row No.	0.001
Formula mean No. of f-valence e^-	0.001
Formula mode groundstate volume per atom	0.001
Formula minimum No. of d-valence e^-	0.001
Tet/Oct E. Differences minimum No. of Unfilled states	0.001
Tetrahedral E. mean Covalent Radius	0.001
Formula minimum No. of f-valence e^-	0.001
Tetrahedral E. mean groundstate volume per atom	0.001
Tet/Oct E. Differences maximum No. of d-unfilled e^-	0.001
Tet/Oct E. Differences mean No. of Valence e^-	0.001
Formula mode No. of d-valence e^-	0.001
Formula maximum Electronegativity	0.001
Formula minimum No. of Valence e^-	0.001

Tetrahedral E. mean No. of Unfilled states	0.001
Tetrahedral E. mode Covalent Radius	0.001
Formula avg. dev. No. of Unfilled states	0.001
Tetrahedral E. mode Atomic Weight	0.001
Tet/Oct E. Differences maximum No. of d-valence e^-	0.001
Tet/Oct E. Differences minimum No. of d-unfilled e^-	0.001
Formula mode No. of f-valence e^-	0.001
Tet/Oct E. Differences maximum No. of Valence e^-	0.001
Tetrahedral E. minimum Atomic Weight	0.001
Tetrahedral E. maximum groundstate volume per atom	0.001
Tetrahedral E. maximum Atomic Weight	0.001
Formula mean No. of Unfilled states	0.001
Tetrahedral E. maximum No. of Unfilled states	0.001
Octahedral E. mode No. of Unfilled states	0.001
Formula minimum Column No.	0.001
Tet/Oct E. Differences mode No. of d-unfilled e^-	0.001
Tet/Oct E. Differences mean No. of d-unfilled e^-	0.001
Tetrahedral E. mean Atomic Weight	0.001
Tetrahedral E. minimum Number	0.001
Octahedral E. maximum No. of Unfilled states	0.001
Tetrahedral E. mean Number	0.001
Tetrahedral E. minimum No. of Unfilled states	0.001
Tetrahedral E. mode No. of Unfilled states	0.001
Octahedral E. maximum Row No.	0.001
Tetrahedral E. maximum Covalent Radius	0.001
Tetrahedral E. maximum Number	0.001
Tetrahedral E. mode No. of Valence e^-	0.001
Formula mean No. of d-unfilled e^-	0.001
Octahedral E. mode Row No.	0.001
Formula avg. dev. Row No.	0.001
Tet/Oct E. Differences maximum No. of Unfilled states	0.001
Tet/Oct E. Differences mean No. of Unfilled states	0.001
Tet/Oct E. Differences minimum Row No.	0.001
Tet/Oct E. Differences mode Row No.	0.001
Tetrahedral E. mode Number	0.001
Octahedral E. mean No. of f-valence e^-	0.001
Formula mode Column No.	0.001
Formula avg. dev. No. of d-valence e^-	0.001
Tetrahedral E. mode No. of d-valence e^-	0.001
Tet/Oct E. Differences maximum Row No.	0.001
Tet/Oct E. Differences minimum No. of d-valence e^-	0.001
Tet/Oct E. Differences mean Row No.	0.001
Formula mode Row No.	0.001
Tetrahedral E. maximum No. of d-valence e^-	0.001
Octahedral E. mode No. of f-valence e^-	0.001
Octahedral E. minimum No. of Unfilled states	0.001
Tet/Oct E. Differences minimum No. of f-valence e^-	0.001
Formula minimum Row No.	0.001
Octahedral E. minimum No. of f-valence e^-	0.001
Tet/Oct E. Differences maximum No. of f-valence e^-	0.001
Tet/Oct E. Differences mode No. of f-valence e^-	0.001
Formula range No. of Unfilled states	0.001
Formula mean groundstate magnetic moment	0.001
Octahedral E. maximum No. of f-valence e^-	0.001

Tetrahedral E. mean No. of d-valence e$^-$	0.001
Formula maximum Row No.	0.001
Tet/Oct E. Differences mean groundstate magnetic moment	0.001
Formula avg. dev. No. of d-unfilled e$^-$	0.001
Tet/Oct E. Differences maximum groundstate magnetic moment	0.001
Tet/Oct E. Differences mean No. of f-valence e$^-$	0.001
Octahedral E. minimum No. of d-unfilled e$^-$	0.001
Formula range Row No.	0.001
Tet/Oct E. Differences mode groundstate magnetic moment	0.001
Tet/Oct E. Differences minimum groundstate magnetic moment	0.001
Octahedral E. maximum No. of d-unfilled e$^-$	0.001
Formula range No. of d-valence e$^-$	0.001
Octahedral E. minimum No. of f-unfilled e$^-$	0.001
Octahedral E. maximum groundstate magnetic moment	0.001
Formula avg. dev. No. of f-unfilled e$^-$	0.001
Formula range groundstate magnetic moment	0.001
Tet/Oct E. Differences maximum No. of s-valence e$^-$	0.001
Octahedral E. mode No. of d-unfilled e$^-$	0.001
Tetrahedral E. mode No. of d-unfilled e$^-$	0.001
Formula maximum No. of d-unfilled e$^-$	0.001
Formula avg. dev. No. of f-valence e$^-$	0.001
Formula minimum No. of Unfilled states	0.001
Octahedral E. mean groundstate magnetic moment	0.001
Tet/Oct E. Differences minimum No. of s-valence e$^-$	0.001
Formula maximum No. of Unfilled states	0.001
Formula maximum groundstate magnetic moment	0.001
Tet/Oct E. Differences mode No. of s-valence e$^-$	0.001

Supplemental table 1: The full list of model features and their importances; there are 233 features with zero importance that are not shown. Feature names containing 'Formula' describe features generated by applying Magpie to the entire 1:1:1 chemical formula. Feature names containing 'Octahedral E.' describe features from applying Magpie to the HH's two octahedrally coordinated elements. Features with 'Tetrahedral E.' are from applying the featurizer to the HH's tetrahedrally coordinated element. Features with 'Tet/Oct E.' are from subtracting 'Octahedral E.' features from 'Tetrahedral E.' for each respective feature.

Here, we discuss our process for determining a cutoff for our ML model's predictions; candidate materials with predicted synthesizabilities above the cutoff are considered synthesizable, and those under the cutoff are considered unsynthesizable. Setting a cutoff too high discards many truly synthesizable candidates, resulting in low recall, while setting the cutoff too low may lead to many truly unsynthesizable candidates, resulting in low precision. In our study, we prioritize precision over recall because 1) false positives are expensive to identify and 2) the number of unreported ABC compositions are in the thousands, so new HHs can likely be found even with low recall.

Precision and recall may be misleading metrics for evaluating suitable cutoffs. If a cutoff at 0.7 corresponds to a precision of 0.8, this means 80% of reported compounds with synthesizabilities greater than 0.7 are synthesizable as HHs. One may determine a cutoff of 0.7 to be sufficient, but imagine if the 80% precision comes from eight HHs with synthesizabilities above 0.9 and two non-HHs with synthesizabilities just above 0.7. In this case, hypothetical compositions near a synthesizability of 0.7 should actually not be recommended since no known HH has a synthesizability near 0.7. This scenario demonstrates how the precision for compositions in the "vicinity" of a given synthesizability may dramatically differ from the precision for all candidates above the given synthesizability. We refer to the precision for compositions near a given synthesizability as the "local precision", which we use to evaluate a suitable cutoff.

We examine cutoffs at multiples of 0.1, and define the local precision as the fraction of compounds with synthesizabilities within $\pm$ 0.05 of each cutoff that are reported as HH. We finalize a cutoff of 0.5 for stable compositions and 0.70 for unstable compositions since the local precisions are respectively ≈ 0.8 (see Supplemental fig. 1), which we accept as sufficiently accurate.

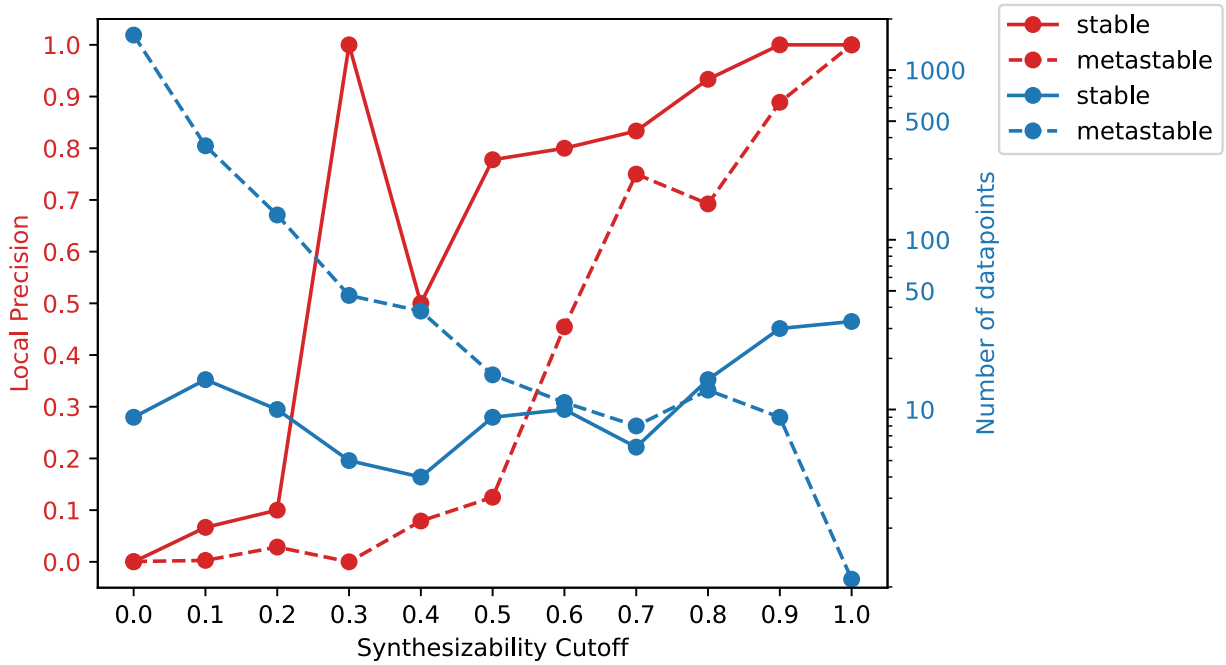

Supplemental fig. 1: Plot of the model's local precision as a function of synthesizability cutoffs. The local precision for a given cutoff is the fraction of reported compounds with synthesizabilities $\pm$ 0.05 of the cutoff that are reported as half-heusler. The number of compounds use to compute local precisions are shown on a secondary axis.

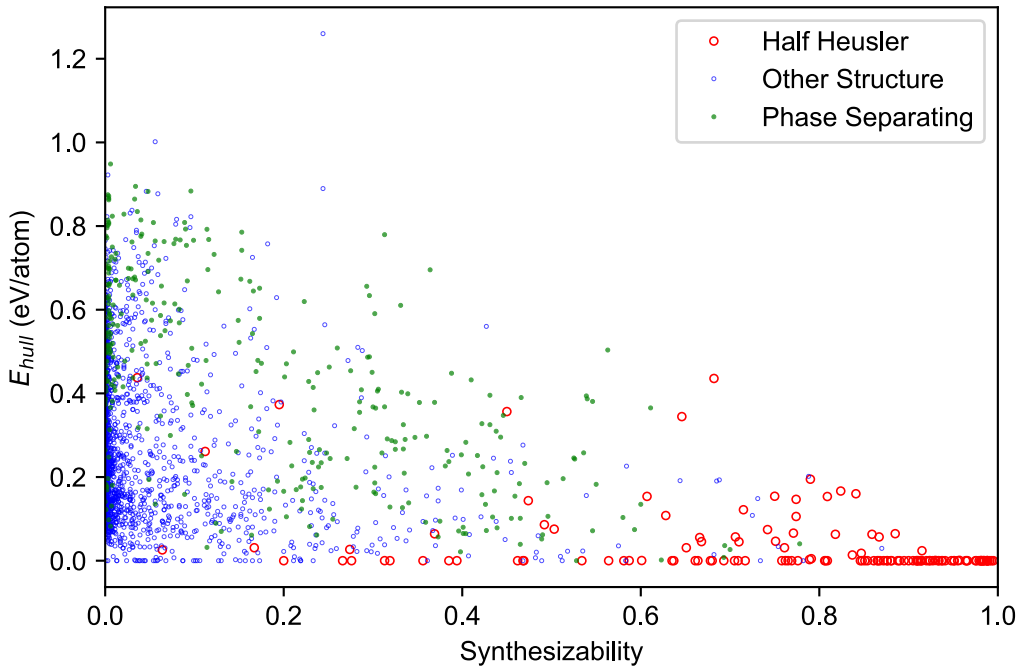

(a) Predictions from a model not trained on phase separating compositions.

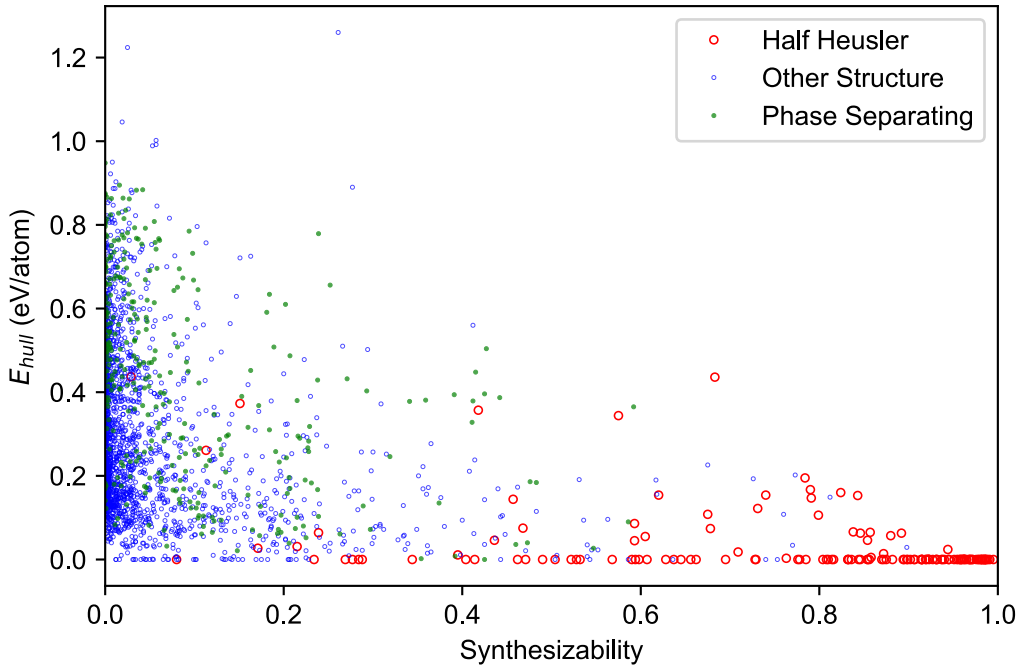

(b) Predictions from a model trained on phase separating compositions.

Supplemental fig. 2: A comparison of synthesizability predictions between a model trained without phase separating compositions (a) and a model that is trained with phase separating compositions (b). On average, the phase separating compositions (green points) in (a) erroneously have higher synthesizabilities than those in (b).

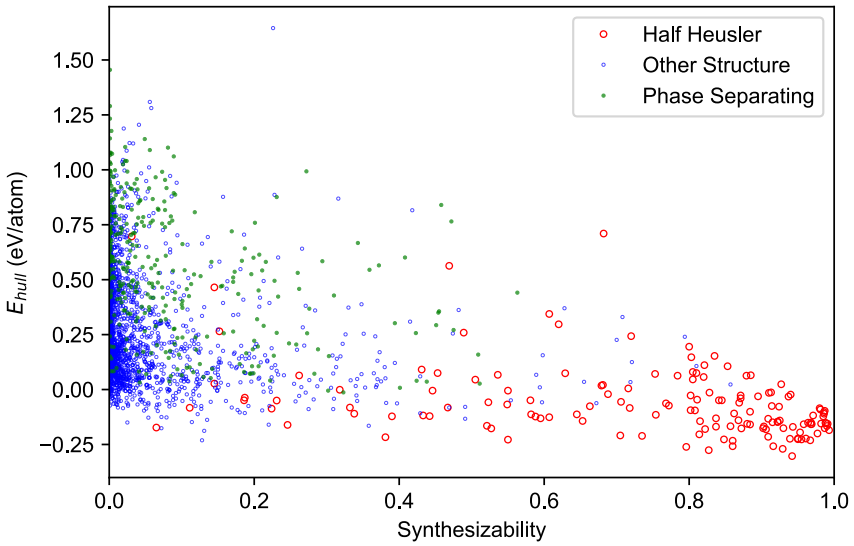

Supplemental fig. 3: Decomposition energies of predictions made by our model on training data points using LOOCV. Decomposition energies are the differences in formation energies between the HH phase and phase separation. Data points are colored according to their labels, as either HH (positive example), other structure (negative example), or phase-separating (negative example). An inverse trend between synthesizability and decomposition energy can be observed, which is in agreement with the general intuition that more-stable compounds are more likely to be synthesizable.

Heusler compounds are class of cubic materials with a large unit cell with 12-16 atomic positions. It could be either thought of as a superstructure of B2 lattice or as a structure composed of two interpenetrating FCC lattices. The Heusler-class of structures contain two octahedrally coordinated sites (X and Z) corresponding to the 4a (0, 0, 0) and 4b ($\frac{1}{2}$, $\frac{1}{2}$, $\frac{1}{2}$) Wyckoff sites, and two tetrahedral sites Y' and Y" corresponding to the 4c ($\frac{1}{4}$, $\frac{1}{4}$, $\frac{1}{4}$) and 4d ($\frac{3}{4}$, $\frac{3}{4}$, $\frac{3}{4}$) Wyckoff sites. If the two octahedral sites are occupied by the same atom the structure becomes B2. In here, we will not consider disorder or intermixing on the octahedral sites, but only occupancy and disorder on the tetrahedral sites.

Table below describes the Heusler class structure designation we use in this paper. The tetrahedral occupancy and disorder described below in most cases noticeably changes the intensities of the diffraction peaks with at least one odd H, K, L in a lattice indexed on space group 216 or 225.

Heusler-type Structure	**Site Occupancy Conditions**
X $= Oct_1$; **Y'** $= Tet_1$; **Y"** $= Tet_2$; **Z** $= Oct_2$ **Half-heusler**: Y' + Y" ≤ 1 ; **Full-heusler**: $1 <$ Y' + Y" ≤ 2	
Half-heusler (HH)	Y' = 1, Y" = 0
Non-stoichiometric half-heusler (NS-HH)	Y' < Y"
Disordered non-stiochiometric half-heusler (DNS-HH)	Y' $\approx$ Y"
Full-heusler (FH)	Y' = 1, Y" = 1
Non-stoichiometric full-heusler (NS-FH)	Y' < Y"
Disordered non-stoichiometric full-heusler (DNS-FH)	Y' $\approx$ Y"

Supplemental table 2: Definitions of various ordered and disordered structures that are considered 'heusler-type'.

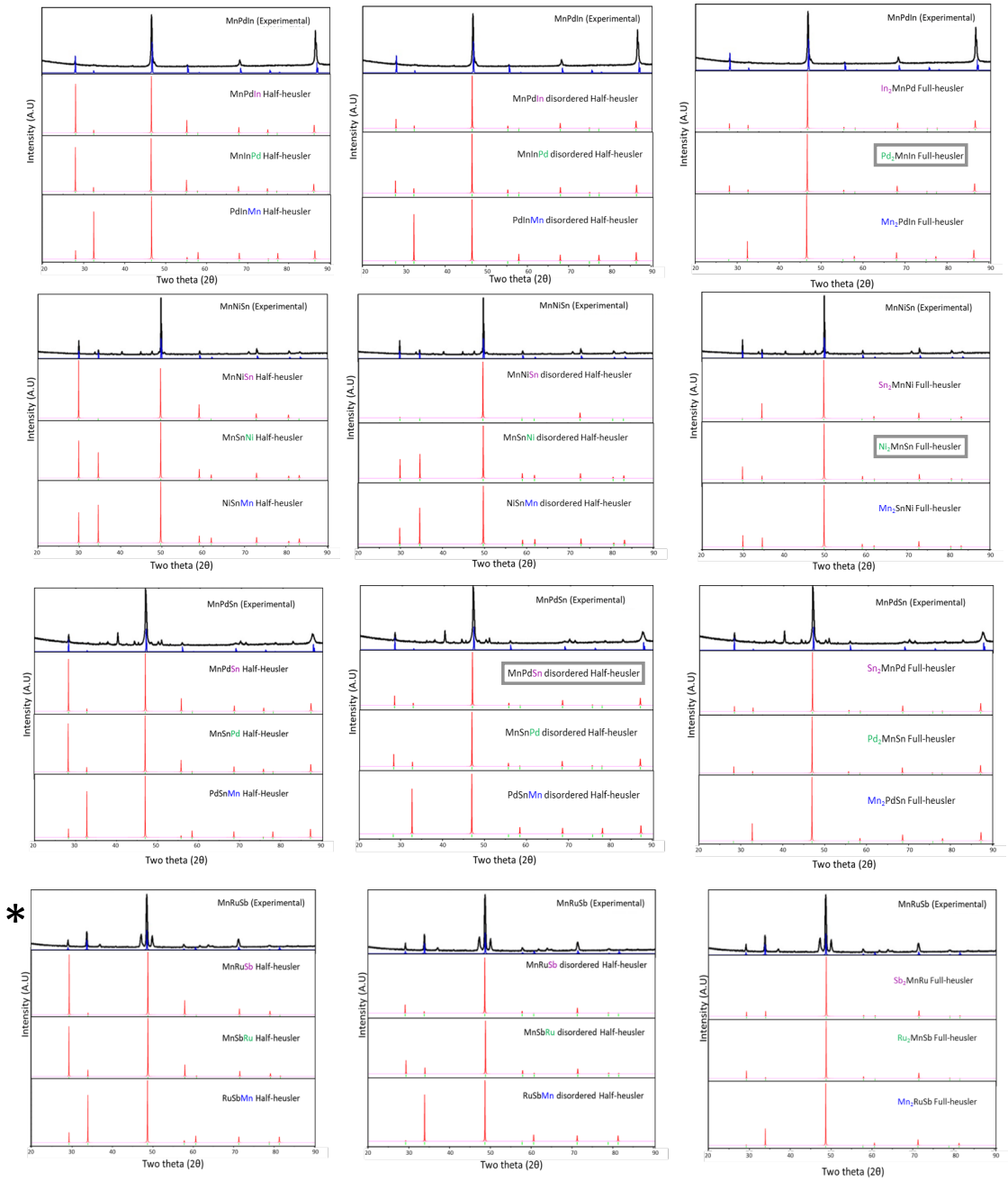

Supplemental fig. 4: Various XRD patterns we simulate (shown in red) for compounds synthesized by Gzyl et al [1] (denoted "Experimental") that are predicted to be HH. Tetrahedrally coordinated elements are colored in each composition label; the structures we identify as the best match to the experimentally reported peaks are boxed in gray. More specific details on site occupancies for the identified disordered structures can be found in Supplemental table 3. * : An additional structure (disordered FH) for MnRuSb is denoted by a * in fig. 5.

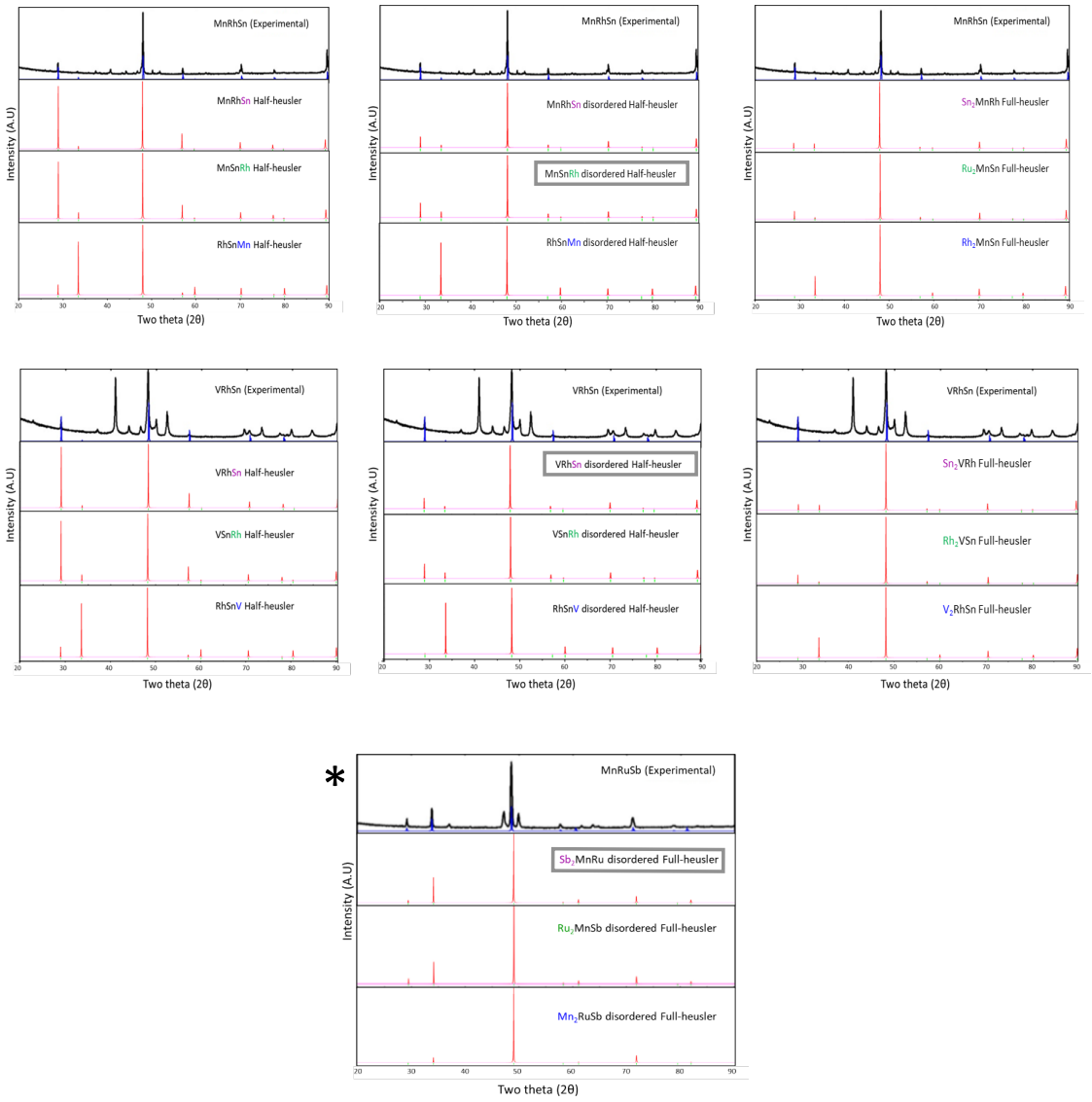

Supplemental fig. 5: Various XRD patterns we simulate (shown in red) for compounds synthesized by Gzyl et al [1] (denoted "Experimental") that are predicted to be HH. Tetrahedrally coordinated elements are colored in each composition label; the structures we identify as the best match to the experimentally reported peaks are boxed in gray. More specific details on site occupancies for the identified disordered structures can be found in Supplemental table 3. An additional structure (disordered FH) for MnRuSb is denoted by *.

Composition	**Observed Primary Phase**	**4a** (0, 0, 0)	**4b** ($\frac{1}{2}$, $\frac{1}{2}$, $\frac{1}{2}$)	**4c** ($\frac{1}{4}$, $\frac{1}{4}$, $\frac{1}{4}$)	**4d** ($\frac{3}{4}$, $\frac{3}{4}$, $\frac{3}{4}$)
MnRhPb	Phase Separated	-	-	-	-
MnPdIn	FH ($MnPd_2In$)	Mn: 1	In: 1	Pd: 1	Pd: 1
MnNiSn	FH ($MnNi_2Sn$)	Mn: 1	Sn: 1	Ni: 1	Ni: 1
MnPdSn	HH (disordered)	Mn: 1	Pd: 1	Sn: 0.5	Sn: 0.5
VRhSn	HH (disordered)	V: 1	Rh: 1	Sn: 0.5	Sn: 0.5
MnRhSn	HH (disordered)	Mn: 1	Sn: 1	Rh: 0.5	Rh: 0.5
MnRuSb	FH (disordered)	Mn: 1	Sb: 1	Ru: 0.5 Mn: 0.25 Sb: 0.25	Ru: 0.5 Mn: 0.25 Sb: 0.25

Supplemental table 3: Site occupancies for the primary phases that we observe with our simulated XRD patterns among compounds that Gzyl et al [1] synthesize. Table headers indicate Wyckoff site positions, and table values indicate the elements and occupancies on each site. When occupancies in a given table cell do not add up to 1, the remaining occupancy fractions can be assumed to belong to vacancies.

Composition	**Convex Hull Decomposition Products**
MnRhPb	MnRh, Pb
MnPdIn	InPd, Mn
MnNiSn	NiSn, Mn
MnPdSn	SnPd, Mn
VRhSn	Sn_2Rh, V_3Rh, Sn_7Rh_5
MnRuSb	Mn, $MnSbRu_2$, Sb_2Ru
MnRhSn	Mn, $MnSnRh_2$, Sn_7Rh_5

Supplemental table 4: Our predictions compared to those made by Gzyl et al for the seven compositions they predict as HH. We simulate XRD patterns (fig. 4 and fig. 5) to identify each compound's primary phase, and calculate the primary phase stabilities. Decompositions products that make up the convex hull at each composition as found in the OQMD are also shown. All compositions are unstable in the HH structure, thus our model considers a composition synthesizable when its synthesizability > 0.75. MnRhPb decomposition products are not reported, thus the stability cannot be calculated. *: multiple phases are observed for all compositions, but only the primary phase is shown here.

Composition	**Experimental Structure**	**Synthesizability**	E_{hull} **(meV/atom) of HH phase**
ScPtBi	Half Heusler (F-43m)	0.941	0
ZrRhBi	Half Heusler (F-43m)	0.901	0
HfIrSb	Half Heusler (F-43m)	0.777	0
ZrIrSb	Half Heusler (F-43m)	0.741	0
TiIrSb	Half Heusler (F-43m)	0.735	0
VRhSn	Phase Separation	0.675	122
ZrIrBi	Half Heusler (F-43m)	0.667	0
TaCoSn	Half Heusler (F-43m)	0.556	0
VIrSn	Phase Separation	0.551	107
ScRhTe	Half Heusler (F-43m)	0.529	0
TaIrSn	Half Heusler (F-43m)	0.481	0
ZrPdPb	Half Heusler (F-43m)	0.476	0
NbCoPb	Phase Separation	0.383	158
ZrNiPb	Half Heusler (F-43m)	0.376	0
MgNiTe	Phase Separation	0.344	120
ScIrTe	Phase Separation	0.317	51
VCoPb	Phase Separation	0.298	370
MgPdS	Phase Separation	0.23	359
InNiBi	Phase Separation	0.191	85
InPdBi	Phase Separation	0.174	50
VIrSi	MgSrSi (Pnma)	0.12	19
MgNiS	Phase Separation	0.104	525
VRhSi	MgSrSi (Pnma)	0.088	135
TiIrP	MgSrSi (Pnma)	0.081	122
HfRhP	MgSrSi (Pnma)	0.056	242
TaIrGe	Half Heusler (F-43m)	0.046	0
AlNiP	Phase Separation	0.035	80
ScPdP	MgSrSi (Pnma)	0.022	191

Supplemental table 5: Summary of compounds synthesized/attempted for synthesis by Gautier et al [2].

Composition	Synthesizability	Composition	Synthesizability
DyPdBi	0.988	HoLiSn*	0.762
YPdBi	0.972	NbFeBi*	0.762
NdPdBi	0.97	TiRuBi*	0.761
ThPtBi	0.952	HfPtBi*	0.76
TiCoBi	0.932	ScCoSb*	0.76
TiRhBi	0.931	ThCoBi	0.757
ScPtBi	0.927	TiIrSb	0.755
SmPtBi	0.922	VPdBi*	0.754
PrPtBi	0.918	MgAuSb	0.752
MgPdBi*	0.916	UNiBi*	0.75
TmAuPb	0.913	MnCuBi*	0.748
LaNiBi	0.91	CrPtBi*	0.747
HfCoBi	0.9	VPtBi*	0.746
YbNiBi*	0.899	TaRhSn	0.746
UPtBi*	0.888	HfRuBi*	0.744
VRhSb*	0.883	MgRhSb	0.743
HfRhBi	0.879	CrNiSb*	0.743
CeNiBi*	0.876	ThCoSb	0.742
UPtSb	0.871	MgAgBi*	0.742
TiNiBi*	0.864	LiTiBi*	0.742
ScRhSb	0.855	VPtSb*	0.741
MnPdBi*	0.851	ZrRuBi*	0.74
ThNiBi*	0.847	NiZnBi*	0.737
ThPdBi*	0.845	CrRuBi*	0.737
NbCoBi*	0.844	MgPtSn	0.735
MnNiBi*	0.839	NiCdBi*	0.73
SmLiSn*	0.838	ULiSn*	0.73
ThPtSb	0.836	MnFeBi*	0.73
NbRuBi*	0.836	ErLiSn*	0.729
LiCdBi*	0.834	ThPdSb*	0.729
UPdBi*	0.834	MnRhSn*	0.728
TiPtSb*	0.833	YbLiSn*	0.728
NiCdSb*	0.831	VIrSb*	0.728
TaRhSb*	0.83	ThLiSn*	0.727
LuAuPb*	0.83	ZrIrSb	0.726
LiCdSb	0.829	NbPtBi*	0.725
VCoBi*	0.824	MnRuBi*	0.724
TaCoBi*	0.823	LiMnBi*	0.724
MnPtBi*	0.823	CrPdSb*	0.724
HfNiBi*	0.822	VFeBi*	0.722
NbRhBi*	0.822	MnCdSb*	0.721
CrRhSb*	0.82	LiCrSb*	0.72
VRhBi*	0.818	ThRhBi	0.72
LiCrBi*	0.818	TaIrSb*	0.719
GdLiSn*	0.818	MnZnBi*	0.719
LaLiSn*	0.81	TaIrBi*	0.717
TaRuBi*	0.804	TaFeBi*	0.715
MgPtBi*	0.803	CrFeBi*	0.714
VNiBi*	0.802	MgCoSb*	0.711
CrRhBi*	0.8	CrFeSb*	0.71
ThNiSb	0.798	LuCoBi*	0.706
LuRhSb	0.798	LuCoSb*	0.706
ZrPtBi*	0.798	NbPtSb*	0.702

MnRhBi*	0.798	MnZnSb*	0.7
CrRuSb*	0.797	HfFeSb	0.699
TiPdSb*	0.797	ZrIrBi	0.682
TaNiSb*	0.797	MgRhBi	0.68
TiPdSn	0.793	MgPdSn	0.656
ScRhBi	0.793	LiAgTe	0.643
MnCoBi*	0.792	MgIrSb	0.64
MnRuSb*	0.791	LiPtSb	0.623
NbNiBi*	0.788	MgAgSn	0.621
MnFeSb*	0.786	NbIrSn	0.612
TbLiSn*	0.786	LiAuBi	0.606
CrNiBi*	0.784	ScIrSb	0.597
TaNiBi*	0.781	ThIrSb	0.584
VRuBi*	0.78	ZrPtPb	0.56
TaFeSb	0.78	ThPdSn	0.544
TiPdBi*	0.777	MgNiSn	0.542
LuRhBi	0.777	LiGaSn	0.528
CuZnSb*	0.777	TaIrSn	0.527
CrPdBi*	0.774	MgPdTe	0.526
CrCoBi*	0.774	AuZnSn	0.525
DyLiSn*	0.772	YbPdTe	0.52
TaRhBi*	0.772	UIrSb	0.52
TiPtBi*	0.772	ScRhTe	0.52
CrCoSb*	0.77	LiCuSb	0.516
NbIrSb*	0.767	ZrRuTe	0.512
NbNiSb*	0.766	ThIrBi	0.512
FeCdSb*	0.764	YRhBi	0.511
HfIrSb	0.764	ThPtPb	0.508
ZrPdBi*	0.764		

Supplemental table 6: List of synthesizable compounds as determined by our model that are unreported in the ICSD, ASM, and SM. DFT unstable compounds are marked with an asterisk (*), and are listed here if their synthesizabilities exceed the cutoff of 0.70. DFT stable compounds are listed here if their synthesizabilities exceed the cutoff of 0.50.

References

[1] A. S. Gzyl, A. O. Oliynyk, and A. Mar, "Half-heusler structures with full-heusler counterparts: Machine-learning predictions and experimental validation," *Crystal Growth & Design*, vol. 20, no. 10, pp. 6469–6477, 2020.

[2] R. Gautier, X. Zhang, L. Hu, L. Yu, Y. Lin, T. O. Sunde, D. Chon, K. R. Poeppelmeier, and A. Zunger, "Prediction and accelerated laboratory discovery of previously unknown 18-electron ABX compounds," *Nature Chemistry*, vol. 7, no. 4, pp. 308–316, 2015.